International Journal of Pharmaceutics 409 (2011) 121–127

Contents lists available at ScienceDirect

International Journal of Pharmaceutics

journal homepage: www.elsevier.com/locate/ijpharm

Hydrogen peroxide mediated transvaginal drug delivery

Hussain Fatakdawala*, Scott A. Uhland

Palo Alto Research Center, 3333 Coyote Hill Rd., Palo Alto, CA 94304, United States

ARTICLE INFO

Article history:
Received 29 October 2010
Received in revised form 25 January 2011
Accepted 21 February 2011

Keywords:
Permeability
Vaginal epithelium
Tight junctions
Hydrogen peroxide
Non-invasive drug delivery

ABSTRACT

Simple, safe and effective permeability enhancers are crucial for successful non-invasive drug delivery methods. We seek local permeability augmentation mechanisms for integration into passive or active architectures in order to enable novel therapeutic delivery routes of the target drug while minimizing drug formulation challenges. This study explores the efficacy of hydrogen peroxide (HP) as a permeability enhancer for transmucosal delivery of macromolecules. HP at low concentrations (2–8 mM) is an effective permeability enhancer that is locally metabolized and safe. HP improves drug permeation through mucosa by altering tight junctions (TJ) between cells and oxidizing enzymes that function to degrade the foreign species. Results from trans-epithelial electrical resistance measurements and cell viability assay show reversible disassembly of TJ with minimal cell damage demonstrating the feasibility of HP as a safe permeability enhancer for drug delivery. Permeation studies show that HP treatment of cell cultured vaginal mucosa significantly enhances the permeability to insulin by more than an order of magnitude. This work lays foundation for the development of a drug delivery platform that administers drug doses by enhancing the permeability of local epithelial tissue via a separate HP treatment step.

1. Introduction

The commercial production of a variety of therapeutic molecules has intensified the study of drug delivery systems to improve bio-availability, therapeutic efficacy, and patient comfort. Efficient drug delivery systems aim at delivering proteins/peptides to the systemic circulation or local tissue via noninvasive routes while maintaining sufficient bio-availability. Many non-invasive drug delivery methods involve overcoming membrane and enzymatic barriers where the underlying principle is to enhance the permeability of the membrane to the target drug. Bio-availability is improved by avoiding first pass metabolism and achieving targeted delivery. In addition, such methods improve patient comfort by reducing the number of doctor visits, avoiding injections and easing administration. Membrane based barriers such as the skin and mucosa have been extensively studied as potential drug delivery routes (Abe et al., 1995; Ackaert et al., 2009; Ahmad et al., 2009; Alur et al., 1999; Ameri et al., 2009; Burkoth et al., 1999; Escobar-Chávez et al., 2009) over the past decade. One such mucosal barrier that has shown great level of interest for both local and systemic delivery is the vaginal epithelium.

Vaginal drug delivery or the delivery of therapeutic molecules across the vaginal mucosa offers numerous advantages such as ease of access, prolonged retention, access to high vasculature, possibility of auto administration and relatively low enzymatic activity. Intra-vaginal drug systems aim at enhancing permeability of the vaginal mucosa to the target drug and therefore provide an alternative administration route for drug therapies. Vaginal drug delivery methods have been studied and developed for treating diseases in women (Bernkop-Schnurch and Hornof, 2003; Mallipeddi and Rohan, 2010; Rohan and Sassi, 2009; Bilensoy et al., 2006) resulting in numerous successful passive approaches to trans-mucosal drug delivery within the female reproductive tract that involve the use of co-formulated solid and semi-solid dosage forms (Acarturk, 2009; das Neves and Bahia, 2006; Madhavlal and Manordas, 2009). Nonetheless, overcoming the challenges associated with simultaneously addressing drug stability and permeability enhancement while maintaining drug bio-availability remains a significant barrier for many therapeutic macromolecules (Bernkop-Schnurch and Hornof, 2003), such as follicle stimulating hormone and parathyroid hormone as well as small molecules such as topotecan hydrochloride. This work focuses on isolating the permeability enhancement methodology from the therapeutic drug in order to minimize many of these technical challenges.

The human vaginal membrane comprises of three layers – mucosa, muscularis and adventitia (Bernkop-Schnurch and Hornof, 2003). The top of the mucosal layer consists of stratified squamous epithelium that acts as the primary barrier to foreign substances. Beneath the epithelial layer exists the lamina propia containing highly vascularized tissue, access to the lymphatic system and nerve fibers. Para-cellular transport across the mucosa is essen-

* Corresponding author. Tel.: +1 732 586 9435.
E-mail addresses: hfatakdawala@ucdavis.edu, hussainkf@gmail.com (H. Fatakdawala), Scott.Uhland@parc.com (S.A. Uhland).

0378-5173/$ – see front matter © 2011 Elsevier B.V. All rights reserved.
doi:10.1016/j.ijpharm.2011.02.052

tially limited due to the inter-cellular apical junctional complex (AJC) that is comprised of tight junctions (TJ) and adherens junctions (AJ) (Ivanov et al., 2005). TJs form the most apical portion of AJC and provide a permeability barrier function while the AJs maintain cell–cell adhesion. The TJs are composed of integral membrane proteins namely occludin and claudins, and peripheral membrane proteins such as zona occludens 1 (ZO-1) and 2 (ZO-2) (Andus and Raub, 1993). These molecules play an important role in maintaining the barrier properties of the junctional complex.

In addition to TJ, the permeation of polypeptides across the mucosa is also impeded by vaginal fluid and mucus layer containing enzymes and macromolecules. Both the pH and volume of vaginal secretions that show considerable variation with time have a profound effect on the bio-availability of the drug. Adequate amounts of fluid (0.5–0.75 mL) (Bernkop-Schnurch and Hornof, 2003), however, may help in solubilizing the drug while pH of the fluid, usually ranging from 4 to 5, affects electrolyte behavior and hence absorption of peptides. Enzymatic activity in the vagina is relatively low, however the presence of nucleases, lysozyme, esterase, guaiacol peroxidase, aldolase and β-glucoronidase in the vaginal fluid do affect drug bio-availability (Bernkop-Schnurch and Hornof, 2003). A primary cause for low bio-availability in vaginally administered protein is the presence of aminopeptidases (Acarturk et al., 2001). The reader is directed to Andus's research (Andus and Raub, 1993) for further detail into the structure and function of the mucosal layer and the composition of the mucus.

HP is known to alter the TJ between epithelial cells (Kevil, 1998) and thereby enhance the permeability of the mucosa to external molecules. The effects of HP on mucosal membranes and the molecular mechanisms involved in the loss of TJs due to HP has been well documented in numerous studies for the gastric (Hashimoto et al., 2008), airway (Hulsmann et al., 1996; Seeger et al., 1995; Waters et al., 1997) and the blood brain barrier epithelium (Kevil et al., 2000; Lee et al., 2004; Schreibelt et al., 2007). Additionally, it has also been reported that alteration to TJ are reversible (Fuller et al., 2007). Specifically, TJ disruption by HP is caused by oxidative stress resulting in the endocytosis of TJ and/or AJ proteins (Ivanov et al., 2005; Utech et al., 2010). The internalized protein either resurfaces back to the membrane or is destroyed by endosomes after removal of the stress. HP is also known to degrade enzymes common to the vaginal tract. The stability of aminopeptidase has been studied in detail by Kuo et al. (2004) using PCR, polyacrylamide gel electrophoresis and Raman spectroscopy. The chemical modification of aminopeptidase by HP was determined to have a profound effect on the protein structure of the enzyme leading to the loss of its catalytic activity.

This paper reports preliminary data on a novel transmucosal drug delivery method that uses HP as a therapeutic permeability enhancer for epithelial tissue by demonstrating reversible TJ disruption with little or no cell death. Studies concentrate on these primary principles in order to enable the development of an innovative drug delivery architecture that first subjects tissue to a permeability enhancing step and then subsequently administers the therapeutic agent. The use of programmable, implantable micro-chip devices (Maloney et al., 2005; Uhland, 2003; Uhland et al., 2004) and micro-electromechanical systems (MEMs) (Ausiello et al., 2004; Prescott et al., 2006) for drug delivery has been demonstrated in our previous work. Such advances in drug delivery device technology will ultimately enable novel drug therapies through miniaturized electrochemical HP generators (Brillas et al., 2002; Gyenge and Oloman, 2005; Gupta and Oloman, 2008; Tatapudi and Fenton, 1993) integrated with microfluidic pumps (Papavasiliou et al., 2000; Bohm et al., 2000; Jackel et al., 1990; Neagu et al., 1996; Xie et al., 2004). Results of this study lay foundation for future in vivo studies focused on designing the prototype architecture to address physical complications associated with vaginal delivery.

2. Materials and methods

2.1. Human vaginal tissue model

The vaginal epithelium was modeled using EpiVaginal™, an *in vitro* epithelial tissue model grown on polycarbonate cell culture tissue inserts by MatTek Corporation (MA, USA). MatTek's vaginal epithelial model has been previously used in drug delivery and toxicity studies (Mesquita et al., 2009; Canny et al., 2006). The tissue model provides an excellent platform that serves as a precursor to human in vivo studies or to entirely avoid animal studies. The tissue samples were provided with Dulbecco's Modified Eagle's Medium (DMEM) for preparation and maintenance of tissue prior to use. Resistance measurements and drug permeation studies were performed using MatTek's VEC-606 tissue platform (tissue area = 4.2 cm^2). VEC-606 tissue inserts were placed on top of a stainless steel washer immersed in 26 ml of DMEM medium in a petri-dish for 2.5 h prior to experimental treatment at 37 °C and humidified 5% CO_2. Tissue/cell viability assay was performed on MatTek's VEC-100 tissue platform (tissue area = 0.5 cm^2) using 5 ml of DMEM medium placed in a cell culture plate. All tissue samples and equipment were handled in a sterile environment in a biosafety cabinet (Labconco Class I/II Laminar Flow Hood with UV sterilization).

2.2. Trans-epithelial electrical resistance (TEER)

Trans-epithelial electrical resistance measurements are widely used to quantitate changes in epithelial permeability. TEER measurements were performed using Millicell ERS 2 system (Millipore Corporation, USA) that is composed of a pair of Ag/AgCl electrodes and a Volt–Ohm meter. The system measures the resistance (0–10,000 Ω, 1 mV/Ω) to ions across the tissue by passing a square wave current (±10 μA, 12.5 Hz). Measurements were performed after addition of 2 ml of the desired concentration of HP solution prepared from 30% stock solution (KMG Electronic Chemicals, TX, USA) into the cell culture insert. The electrodes were clamped in place in an incubator (37 °C and humidified 5% CO_2) and data was collected automatically using LabView data acquisition software. Data points were acquired every 30 min and the electrodes were switched 'off' between measurements using a LabView triggered relay switch to avoid incurring damage to tissue. The HP solution was removed after 5 h and the tissue inserts were rinsed with PBS and incubated to allow recovery. The data was collected automatically for 5 h and the end data points (24 h) were manually measured.

2.3. 3-(4,5-Dimethythiazol-2-yl)-2,5-diphenyl tetrazolium bromide (MTT) assay

MTT assay was used to quantitate any detrimental effects on the tissue due to HP treatments. The assay kit was purchased from MatTek Corp. (MTT-100). The HP treatment solution was tested and found not to interfere with the assay. The assay was performed as outlined in MatTek Corp.'s MTT effective time-50 (ET-50) protocol. Post-treatment with the desired HP dose (100 μl), the tissue inserts were rinsed twice with PBS to remove any residual HP. The negative control comprised of untreated tissue while the positive control was treated with 100 μl of 1% Triton-X. The inserts were incubated in 300 μl of 1 mg/ml MTT solution for 3 h at 37 °C. The inserts were then transferred into 1.66 ml of extraction solution and incubated overnight at room temperature. The optical density (OD) of the extractant was measured at 570 nm. The % viability of

epithelial cells was calculated as follows:

$$\%\ \text{viability} = \frac{\text{OD}_{\text{sample}}}{\text{OD}_{\text{negative control}}} \times 100 \quad (1)$$

2.4. Immunofluorescence

Immunofluorescence samples were prepared in a similar fashion as described in Tang (2006). Prior to fixation, the tissue inserts were chilled at 4 °C for 3 h and then rinsed five times with antibody diluent (1% bovine serum albumin, 10 mM PBS, 0.05% sodium azide, pH 7.5) at 4 °C. The inserts were immediately fixed in 100% methanol at −20 °C for atleast 18 h and then rinsed briefly with 100% acetone and air dried at room temperature. The tissue was excised from the inserts and placed into a multiwell plate and rinsed twice with antibody diluent. The primary antibody (ab31721, rabbit polyclonal to occludin, Abcam Inc.) was incubated in the same diluent overnight at room temperature. Following incubation, the tissue was washed 3 times and incubated with the secondary antibody (ab6564, Goat polyclonal to Rabbit IgG – H&L (Cy5), Abcam Inc.) at room temperature for 3 h. The tissue was then washed 6 times and fixed in 100% ethanol for 3 h at −20 °C and air dried. All washes were performed using the antibody diluent at 4 °C. Tissue samples were mounted on to a slide using ProLong Gold anti-fade reagent (Molecular Probes) with coverslip on top. Images were obtained from Zeiss 510 UV/vis Meta laser scanning confocal microscope (University of California, Berkeley).

2.5. Preliminary drug permeation study

We explored the permeability of bovine insulin (Sigma–Aldrich) across the vaginal epithelium after treatment with different concentrations of HP for varying exposure times. HP solutions were prepared from 30% stock solution (KMG Electronic Chemicals, TX, USA). Following pre-treatment, 5 ml of the desired concentration of HP solution was added to the inserts. All HP doses are reported in terms of μmol per unit area of tissue (μmol/cm^2). After the HP treatment, the inserts were carefully washed using phosphate buffered saline (PBS) (Sigma–Aldrich) and introduced into Nunc™ culture plate wells containing 5 ml of bovine serum (BS) (Sigma–Aldrich). 1 ml of the insulin drug solution (200 ng/ml) was placed on top of the tissue surface and the setup was agitated at 120 rpm. Positive control comprised of a blank insert (no tissue) while the negative control included an untreated tissue sample. Permeation of the same drug concentration was studied for both the positive and the negative control.

2.6. Drug characterization

20 μl of the BS from the plate was sampled at different time points for quantitative analysis for the presence of the drug. Insulin ELISA Kit (ALPCO Diagnostics, Bovine Insulin ELISA) was used to determine the concentrations of insulin in the samples aliquoted. The ELISA procedure was followed as outlined in the kit protocol.

2.7. HP degradation and characterization

The degradation of HP due to tissue was studied by comparing HP neutralization rates in the presence and absence of tissue. HP concentrations for the degradation study were determined using a peroxide assay kit – PeroXOquant (Thermo Scientific, Pierce Protein Research Products, IL, USA). Samples were aliquoted and immediately analyzed. Assay was performed using the protocol supplied with the kit.

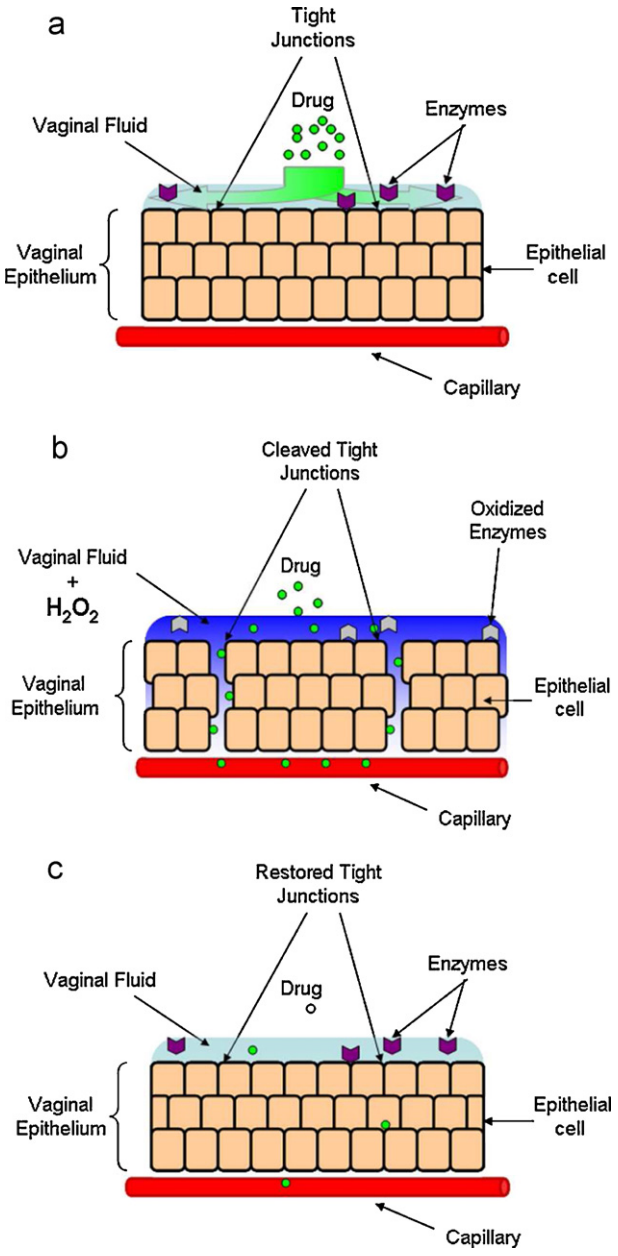

Fig. 1. (a) The initial state of vaginal epithelial permeability barriers, (b) application of HP and the mechanism(s) for increased drug permeability and (c) the recovery of the tight junction barrier after HP neutralization.

3. Results and discussion

The experimental results demonstrate the potential of HP as a permeability enhancer and its effects on human vaginal epithelium for drug delivery. The overall concept of HP as a permeability enhancer is summarized in Fig. 1. HP enhances permeability of vaginal epithelium by disrupting TJ between cells and reducing the effect of enzymes (such as aminopeptidase) locally (Kuo et al., 2004).

3.1. TEER and immunofluorescence measurements

Immunofluorescence results for TJ disassembly and recovery are shown in Fig. 2 via immunofluorescent staining of occludin, a specific transmembrane protein found in TJs. Results depict the disassembly/dislocation of occludin after HP treatment and also

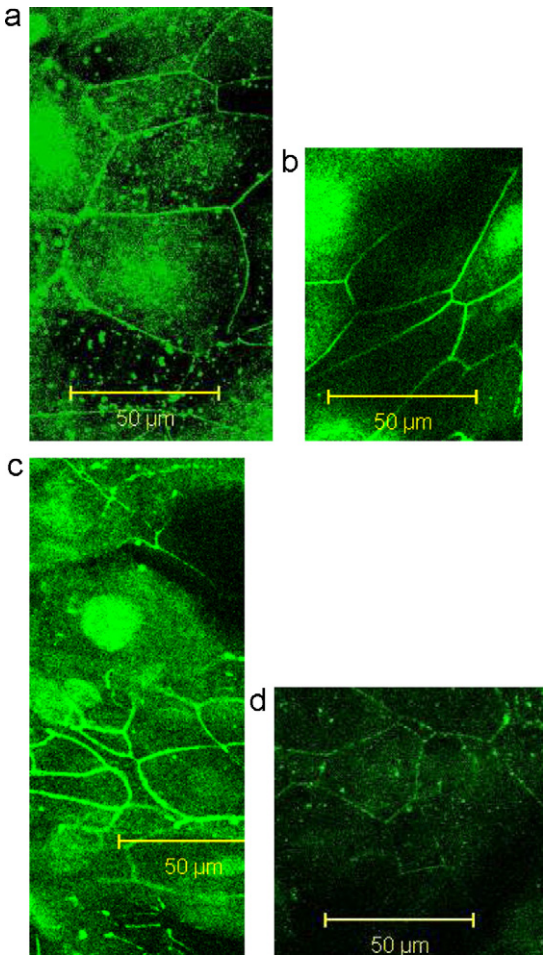

Fig. 2. Immunofluorescence staining of occludin protein in human vaginal epithelial cells. Tissue was treated with primary antibody – rabbit polyclonal to occludin, Abcam Inc. and secondary antibody – Goat polyclonal to Rabbit IgG – H&L (Cy5), Abcam Inc. (a) Negative control, (b) 2 h treatment with HP dose of 8 μmol/cm^2. Recovery after treatment with HP dose of (c) 8 μmol/cm^2 and (d) 24 μmol/cm^2.

the recovery of the same after removal of the dose. Compromise in TJ assembly is seen as discontinuity in fluorescence around cell boundaries. Staining results show disassembly and recovery of TJs for the 8 μmol/cm^2 HP dose treatment. Recovery was not observed for the 24 μmol/cm^2 dose treatment. TEER results are summarized in Fig. 3. HP doses ranging from 2.4 to 16 μmol/cm^2 were effective in reversibly reducing the TEER of the tissue samples. TEER recovery was observed within 24 h after removal of the HP solution. All HP doses initiate a rapid drop in TEER within the first 30 min of the treatment time as observed from Fig. 3. This indicates that the effect of HP on tissue is rapid and that HP is readily consumed over tissue (HP degradation is discussed in Section 3.2). Higher doses (20 and 24 μmol/cm^2) however, did not show recovery indicating that majority of TJ and/or AJC function was lost.

Fig. 4 summarizes the change in energy (ΔE) for different HP dose treatments. ΔE values were computed using the following relation:

$$\Delta E = i^2(R - R_0)t \quad (2)$$

where i is the applied current (10 μA), R is the TEER value and t is the duration of TEER measurement for each data point. The calculation was performed using data representing the 5 h treatment. ΔE values increase steadily with doses up to 16 μmol/cm^2. 20 and 24 μmol/cm^2 doses however, show a higher increase (double) in ΔE compared to the 16 μmol/cm^2 dose. This suggests that

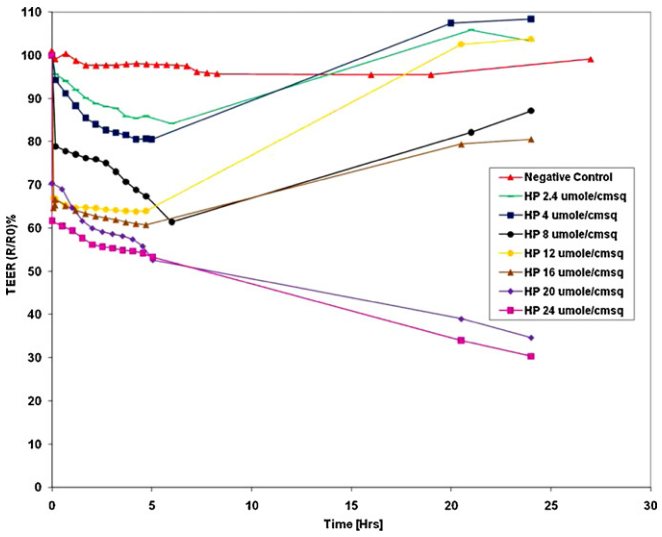

Fig. 3. TEER of human vaginal epithelia in response to different HP dose treatments (μmol/cm^2).

the higher doses induce an additional chemical/physical change in tissue rendering slow to no recovery of TJ function. ΔE is attributed to the energy involved in the HP–tissue interaction, majority of which involves TJ disassembly, ultimately enabling the permeation of water soluble species.

Utech et al. have shown that oxidative stress causes internalization of TJ and/or AJC proteins (Ivanov et al., 2005; Utech et al., 2010) lowering TEER. The absence of TEER recovery at higher HP doses is due to higher oxidative stresses preventing resurfacing of TJ proteins that were internalized. Meyer et al. (2001) demonstrated that reassembly of TJs does not involve the synthesis of new proteins but is accomplished via re-utilization of existing proteins particularly tyrosine kinases. Higher oxidative stresses inactivate kinase activity (Tang et al., 2005) thereby preventing TJ re-assembly.

3.2. HP degradation study

HP is a semi-stable oxidizing weak base that readily decomposes into water and oxygen following the thermodynamically favorable reaction:

$$2H_2O_2 \rightarrow 2H_2O + O_2 \quad (3)$$

Fig. 5 summarizes HP degradation with and without tissue during incubation. The degradation of HP during incubation (37 °C and humidified 5% CO_2) was studied and the intrinsic neutralization rate of HP was found to be 2 μmol/cm^2/h. The rate of neutralization increased to 11.5 μmol/cm^2/h when incubated in the presence of vaginal epithelial tissue. The rate of HP neutralization over tis-

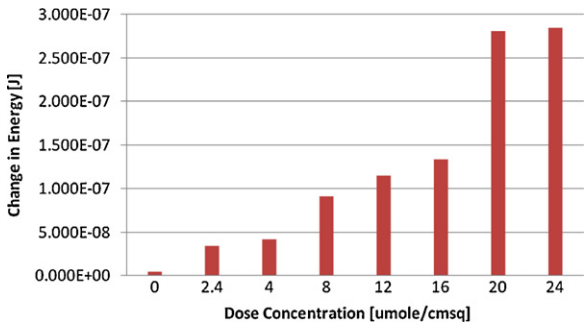

Fig. 4. Change in energy with time computed from TEER results for various HP treatments (μmol/cm^2).

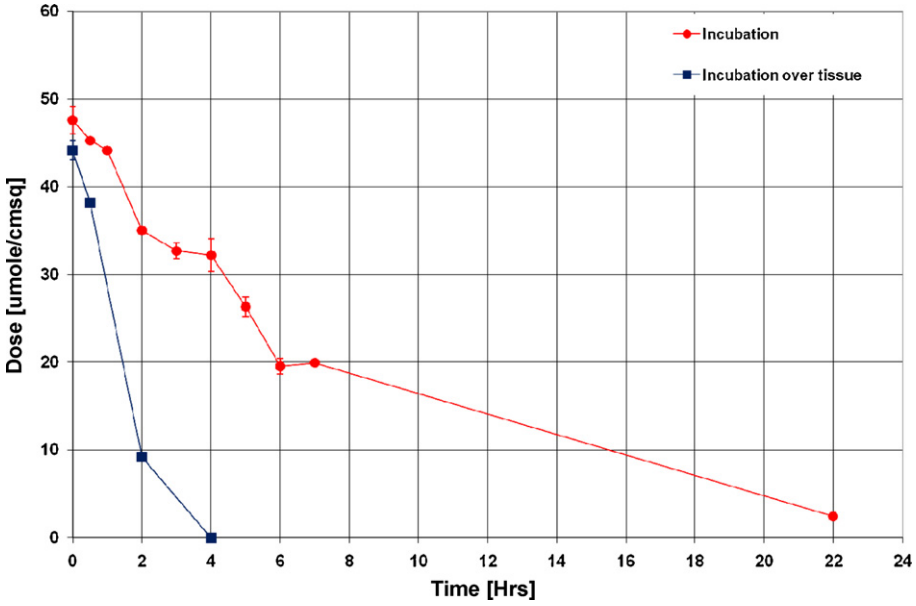

Fig. 5. HP degradation during incubation (37 °C and humidified 5% CO_2) with and without tissue. Vaginal epithelial tissue was found to greatly accelerate degradation of HP.

sue correlates with the rapid initial drop in TEER due to HP induced oxidative stress. HP neutralization results also demonstrate that nearly all of HP dose is neutralized within the first hour of treatment during TEER measurements. However, TEER continues to drop beyond the first hour indicating a post treatment effect. The effect may be due to low residual HP, HP induced alterations in local pH and elevated oxygen levels. The post treatment effect generates similar TEER reduction rates across all dose treatments (see Fig. 3). HP degradation is attributed to enzymatic activity i.e. peroxiredoxin-2 and thioredoxin of tissue (O'Hanlon et al., 2010; Quinzio et al., 2008) and/or chemical decomposition during incubation in addition to interaction with tissue. The rapid degradation of HP is an important criterion for its use as a safe permeability enhancer as dose concentrations up to 45 μmol/cm^2 have a fairly low residence time over tissue (see Fig. 5). TEER and HP neutralization results confirm that the initial permeability enhancement is accompanied with neutralization of majority of the HP dose and that tissue recovery begins with in the 5 h treatment. This implies that the target drug may be dispensed after 15–20 min from start of treatment for the HP doses outlined in the TEER experiments. These time scales are essential in guiding future in vivo work to determine the synchronization of HP treatment and subsequent drug dosing.

3.3. MTT assay

Results from the MTT assay are shown in Fig. 6. The assay results show that the HP treatments with doses up to 24 μmol/cm^2 do not cause any significant damage to the tissue. Doses ranging from 2.4 to 16 μmol/cm^2 (all results not shown) did not cause any measurable cell death while 24 μmol/cm^2 dose induced slight tissue damage. 100 μmol/cm^2 dose however, caused significant damage to tissue reducing viability to 50% within 12 h. Assay and TEER results indicate that there exists a wide range of HP dose concentrations that can effectively disassemble TJ without causing significant cell death. Cell death due to HP may be caused due to damage to DNA. HP induced DNA damage has been demonstrated in respiratory epithelia (McDonald et al., 1993). Cell death due to oxidative stress has been attributed to apoptosis or necrosis or both. While apoptosis results due to damage to nuclear proteins, necrosis occurs due to damage to organelles and loss of plasma-membrane. Kim et al. (2003) demonstrated retinal pigment epithelial cell death via apoptosis at low HP concentrations and necrosis at high HP concentrations. HP induced vaginal epithelial cell death was observed to be less fatal, and is attributed to the existence of 10–16 layers of cells (compared to results from a monolayer) and rapid neutralization of HP.

3.4. Preliminary drug permeation study

The permeation results for insulin across the vaginal epithelium are shown in Fig. 7. The 2 h, 2.4 μmol/cm^2 dose of HP treatment was successful in permeating insulin across the epithelia, which is the lowest dose that achieves reversible TJ disassembly with no tissue damage. The integrated flux of insulin across epithelia was comparable to the positive control. Negative control results demonstrate that insulin permeation across epithelia is solely due to HP treatment. Although a 2 h treatment is required, HP degradation results show that the drug can be introduced over tissue within 15–20 min of treatment without HP induced damage to the drug. TEER results show that resistance to ionic flow decreases rapidly and continues to decrease up to 5 h due to post treatment effects. The increase in

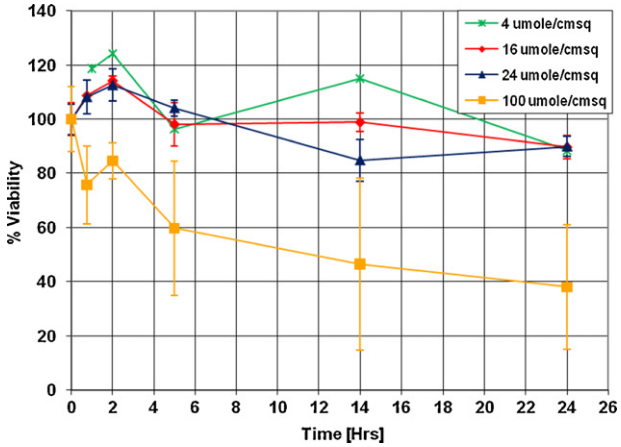

Fig. 6. % viability of human vaginal epithelium after exposure to varying HP doses (μmol/cm^2) as determined by the MTT assay.

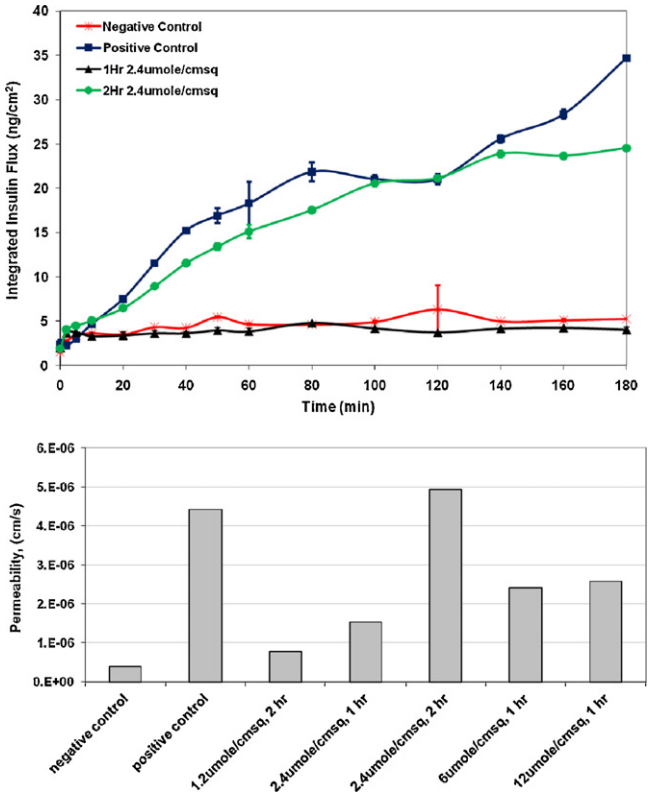

Fig. 7. (a) Integrated insulin flux (ng/cm^2) across vaginal epithelium and (b) the calculated permeability (cm/s) for different HP concentrations and treatment durations (HP dose [μmol/cm^2], treatment time [h]).

2.4 μmol/cm^2 HP treatment time required to achieve insulin permeation relative to the TEER observations at 2.4 μmol/cm^2 is likely a result of larger size of the insulin molecule.

The permeability values (P_{total}) were calculated from the following relation:

$$J = \frac{\Delta M}{\Delta t}, \tag{4}$$

$$P_{total} = \frac{J}{\Delta C}. \tag{5}$$

where ΔJ is the transmucosal flux (ng/cm^2/s), ΔM is the measured drug mass transported per unit area of tissue during time Δt, ΔC is the concentration difference across the tissue and P_{total} is the total permeability (cm/s) of the tissue platform (the tissue and its polycarbonate membrane support). Permeability values show that both HP dose concentrations and treatment durations can be employed in controlling epithelial permeability. TEER results also demonstrate that higher HP doses and longer treatment durations allow higher permeability enhancement, where dose concentrations dictate the initial drop in TEER and treatment duration allow further drop in TEER due to post treatment effects.

The epithelial tissue and the polycarbonate membrane tissue culture support can be treated as resistors/barriers in series (Fig. 8(a)) in order to understand the time scale of drug permeation through the tissue. The total permeability can be represented as follows:

$$\frac{1}{P_{total}} = \frac{1}{P_{tissue}} + \frac{1}{P_{membrane}}, \tag{6}$$

where P_{tissue} is the tissue permeability and $P_{membrane}$ is the permeability of the porous polycarbonate membrane support. The permeability of the epithelial tissue can be computed by subtracting the permeability result of the positive control (blank insert).

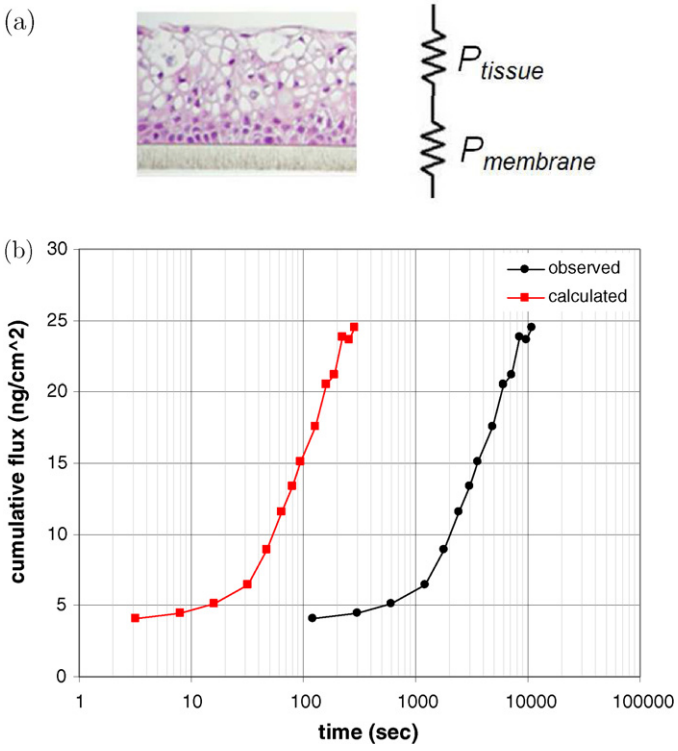

Fig. 8. (a) The epithelia and the polycarbonate membrane can be treated as resistors in series. (b) Observed vs. calculated insulin flux for 2 h, 2.4 μmol/cm^2 HP treatment.

Assuming steady state conditions, the permeation time through the tissue is then determined as follows:

$$t_{tissue} = \frac{P_{total}}{P_{tissue}} \times t_{measured} \tag{7}$$

where $t_{measured}$ is the observed time during the permeation studies. The resulting calculated insulin flux profile through the tissue is compared to the observed insulin flux in Fig. 8(b). This result shows that up to 200 ng of insulin can be administered across the epithelia in approximately 5 min.

4. Conclusions

Experimental results have shown that HP can reversibly disassemble TJ barrier functions between epithelial cells over a fairly broad range of dose concentrations (2.4–16 μmol/cm^2) with minimal to no cell/tissue damage thereby safely enhancing the permeability of vaginal mucosa to macromolecules. Tissue damage was observed only for a high HP dose treatment of 100 μmol/cm^2. Additionally, HP was found to neutralize rapidly over tissue implying that the residence time of HP over tissue is fairly short. This enables HP to drive a permeability enhancement step separate from the target drug avoiding formulation and drug stability issues. The study of HP neutralization is important for future work in in vivo studies for estimating the required critical time lapse between HP treatment and drug administration. The drug can then be dispensed after HP degrades to safe critical dose. A low HP dose treatment (2.4 μmol/cm^2) was successful in permeating insulin across vaginal epithelium over a period of 5–10 min. Results of this study establish the foundation for the development of a novel vaginal drug delivery architecture that uses HP to enhance permeability of local vaginal tissue followed by accurate administration of therapeutics. This platform offers a promising new drug delivery route that can be employed for treatment of a variety of diseases within women's health, such as infertility treatment via fertility hormones, osteoporosis management via parathyroid hormone administration and

cancers of the reproductive tract via chemotherapy. Future work will be focused on in vivo studies assessing the safety effects of HP as a permeability enhancer on tissue and the resulting pharmacokinetics of HP mediated vaginal drug delivery.

References

Abe, K., Irie, T., Uekama, K., 1995. Enhanced nasal delivery of luteinizing hormone releasing hormone agonist buserelin by oleic acid solubilized and stabilized in hydroxypropyl-beta-cyclodextrin. Chem. Pharm. Bull. (Tokyo) 43, 2232–2237.

Acarturk, F., 2009. Mucoadhesive vaginal drug delivery systems. Recent Patents Drug Deliv. Formul. 3, 193–205 (13).

Acarturk, F., Parlatan, Z.I., Saracoglu, O.F., 2001. Comparison of vaginal aminopeptidase enzymatic activities in various animals and in humans. J. Pharm. Pharmacol. 53, 1499–1504.

Ackaert, O.W., Smeden, J.V., Graan, J.D., Dijkstra, D., Danhof, M., Bouwstra, J.A., 2009. Mechanistic studies of the transdermal iontophoretic delivery of 5-oh-dpat in vitro. J. Pharm. Sci..

Ahmad, Z., Stride, E., Edirisinghe, M., 2009. Novel preparation of transdermal drug-delivery patches and functional wound healing materials. J. Drug Target 17, 724–729.

Alur, H.H., Pather, S.I., Mitra, A.K., Johnston, T.P., 1999. Transmucosal sustained-delivery of chlorpheniramine maleate in rabbits using a novel, natural mucoadhesive gum as an excipient in buccal tablets. Int. J. Pharm. 188, 1–10.

Ameri, M., Daddona, P., Maa, Y.F., 2009. Demonstrated solid-state stability of parathyroid hormone pth(1-34) coated on a novel transdermal microprojection delivery system. Pharm. Res..

Andus, K.L., Raub, T.L. (Eds.), 1993. Biological Barriers to Protein Delivery. Pharmaceutical Biotechnology, vol. 4. Springer.

Ausiello Jr., D., Santini, J.T., Herman, S.J., Prescott, J.H., 2004. Method and device for the controlled delivery of parathyroid hormone.

Bernkop-Schnurch, A., Hornof, M., 2003. Intravaginal drug delivery systems: design, challenges, and solutions. Am. J. Drug Deliv. 1, 241–254 (14).

Bilensoy, E., Rouf, M.A., Vural, I., Sen, M., Hincal, A.A., 2006. Mucoadhesive, thermosensitive, prolonged-release vaginal gel for clotrimazole:beta-cyclodextrin complex. AAPS PharmSciTech 7, E38.

Bohm, S., Olthuis, W., Bergveld, P., 2000. A bi-directional electrochemically driven micro liquid dosing system with integrated sensor/actuator electrodes. In: Thirteenth International Conference on Micro Electro Mechanical Systems, IEEE , Miyazaki, Japan.

Brillas, E., Alcaide, F., Cabot, P.L., 2002. A small-scale flow alkaline fuel cell for on-site production of hydrogen peroxide. Electrochim. Acta 48, 331–340.

Burkoth, T.L., Bellhouse, B.J., Hewson, G., Longridge, D.J., Muddle, A.G., Sarphie, D.F., 1999. Transdermal and transmucosal powdered drug delivery. Crit. Rev. Ther. Drug Carrier Syst. 16, 331–384.

Canny, G.O., Trifonova, R.T., Kindelberger, D.W., Colgan, S.P., Fichorova, R.N., 2006. Expression and function of bactericidal/permeability-increasing protein in human genital tract epithelial cells. J. Infect. Dis. 194, 498–502.

das Neves, J., Bahia, M., 2006. Gels as vaginal drug delivery systems. Int. J. Pharm. 318, 1–14.

Escobar-Chávez, J.J., Bonilla-Martínez, D., Villegas-González, M.A., Revilla-Vázquez, A.L., 2009. Electroporation as an efficient physical enhancer for skin drug delivery. J. Clin. Pharmacol. 49, 1262–1283.

Fuller, E., Duckham, C., Wood, E., 2007. Disruption of epithelial tight junctions by yeast enhances the paracellular delivery of a model protein. Pharm. Res. 24, 37–47.

Gupta, N., Oloman, C., 2008. Modeling a perforated bipole trickle bed electrochemical reactor for the generation of alkaline peroxide. J. Appl. Electrochem. 38, 131–149, doi:10.1007/s10800-007-9411-4.

Gyenge, E.L., Oloman, C.W., 2005. The surfactant-promoted electroreduction of oxygen to hydrogen peroxide. J. Electrochem. Soc. 152, D42–D53.

Hashimoto, K., Oshima, T., Tomita, T., Kim, Y., Matsumoto, T., Joh, T., Miwa, H., 2008. Oxidative stress induces gastric epithelial permeability through claudin-3. Biochem. Biophys. Res. Commun. 376, 154–157.

Hulsmann, A., Raatgeep, H., den Hollander, J., Bakker, W., Saxena, P., de Jongste, J., 1996. Permeability of human isolated airways increases after hydrogen peroxide and poly-L-arginine. Am. J. Respir. Crit. Care Med. 153, 841–846.

Ivanov, A.I., Nusrat, A., Parkos, C.A., 2005. Endocytosis of the apical junctional complex: mechanisms and possible roles in regulation of epithelial barriers. Bioessays 27, 356–365.

Jackel, J.L., Johnson, J.J., Tomlinson, W.J., 1990. Bistable optical switching using electrochemically generated bubbles. Opt. Lett. 15, 1470–1472.

Kevil, C.G., 1998. Effects of Hydrogen Peroxide on Endothelial Adherens and Tight Junctional Structure and Barrier Function In Vitro. Louisiana State University Medical Center, Shreveport.

Kevil, C.G., Oshima, T., Alexander, B., Coe, L.L., Alexander, J.S., 2000. H_2O_2-mediated permeability: role of MAPK and occludin. Am. J. Physiol. Cell Physiol. 279, C21–C30, http://ajpcell.physiology.org/cgi/reprint/279/1/C21.pdf.

Kim, M.H., Chung, J., wook Yang, J., Chung, S.M., Kwag, N.H., Yoo, J.S., 2003. Hydrogen peroxide-induced cell death in a human retinal pigment epithelial cell line, arpe-19. Korean J. Ophthalmol. 17, 19–28.

Kuo, L.Y., Hwang, G.Y., Yang, S.L., Hua, Y.W., Chen, W., Lin, L.L., 2004. Inactivation of bacillus stearothermophilus leucine aminopeptidase ii by hydrogen peroxide and site-directed mutagenesis of methionine residues on the enzyme. Protein J. 23, 295–302.

Lee, H.S., Namkoong, K., Kim, D.H., Kim, K.J., Cheong, Y.H., Kim, S.S., Lee, W.B., Kim, K.Y., 2004. Hydrogen peroxide-induced alterations of tight junction proteins in bovine brain microvascular endothelial cells. Microvasc. Res. 68, 231–238.

Madhavlal, P.G., Manordas, P.M., 2009. Design and in vitro evaluation of a novel vaginal drug delivery system based on gelucire. Curr. Drug Deliv. 6, 159–165.

Mallipeddi, R., Rohan, L.C., 2010. Nanoparticle-based vaginal drug delivery systems for hiv prevention. Exp. Opin. Drug Deliv. 7, 37–48.

Maloney, J.M., Uhland, S.A., Polito, B.F., Sheppard Jr., N.F., Pelta, C.M., Santini Jr., J.T., 2005. Electrothermally activated microchips for implantable drug delivery and biosensing. Proceedings of the Twelfth International Symposium on Recent Advances in Drug Delivery Systems. J. Control. Release 109, 244–255.

McDonald, R.J., Pan, L.C., George, J.A.S., Hyde, D.M., Ducore, J.M., 1993. Hydrogen peroxide induces dna single strand breaks in respiratory epithelial cells. Inflammation 17, 715–722.

Mesquita, P.M.M., Cheshenko, N., Wilson, S.S., Mhatre, M., Guzman, E., Fakioglu, E., Keller, M.J., Herold, B.C., 2009. Disruption of tight junctions by cellulose sulfate facilitates hiv infection: model of microbicide safety. J. Infect. Dis. 200, 599–608.

Meyer, T.N., Schwesinger, C., Ye, J., Denker, B.M., Nigam, S.K., 2001. Reassembly of the tight junction after oxidative stress depends on tyrosine kinase activity. J. Biol. Chem. 276, 22048–22055.

Neagu, C.R., Gardeniers, J.G., Elwenspoek, M., Kelly, J.J., 1996. An electrochemical microactuator: principle and first results. J. Microelectromech. Syst. 5, 2–9.

O'Hanlon, D.E., Lanier, B.R., Moench, T.R., Cone, R.A., 2010. Cervicovaginal fluid and semen block the microbicidal activity of hydrogen peroxide produced by vaginal lactobacilli. BMC Infect. Dis. 10, 120.

Papavasiliou, A.P., Liepmann, D., Pisano, A.P., 2000. Electrolysis-bubble actuated gate valve. In: Solid-State Sensor and Actuator Workshop.

Prescott, J.H., Lipka, S., Baldwin, S., Sheppard, N.F., Maloney, J.M., Coppeta, J., Yomtov, B., Staples, M.A., Santini, J.T., 2006. Chronic, programmed polypeptide delivery from an implanted, multireservoir microchip device. Nat. Biotechnol. 24, 437–438.

Quinzio, M.K.W.D., Georgiou, H.M., Holdsworth-Carson, S.J., Ayhan, M., Heng, Y.J., Walker, S.P., Rice, G.E., Permezel, M., 2008. Proteomic analysis of human cervicovaginal fluid displays differential protein expression in association with labor onset at term. J. Proteome Res. 7, 1916–1921.

Rohan, L.C., Sassi, A.B., 2009. Vaginal drug delivery systems for hiv prevention. AAPS J. 11, 78–87.

Schreibelt, G., Kooij, G., Reijerkerk, A., van Doorn, R., Gringhuis, S.I., van der Pol, S., Weksler, B.B., Romero, I.A., Couraud, P.O., Piontek, J., Blasig, I.E., Dijkstra, C.D., Ronken, E., de Vries, H.E., 2007. Reactive oxygen species alter brain endothelial tight junction dynamics via RhoA, PI3 kinase, and PKB signaling. FASEB J. 21, 3666–3676, http://www.fasebj.org/cgi/reprint/21/13/3666.pdf.

Seeger, W., Hansen, T., Rössig, R., Schmehl, T., Schütte, H., Krämer, H.J., Walmrath, D., Weissmann, N., Grimminger, F., Suttorp, N., 1995. Hydrogen peroxide-induced increase in lung endothelial and epithelial permeability-effect of adenylate cyclase stimulation and phosphodiesterase inhibition. Microvasc. Res. 50, 1–17.

Tang, H., Hao, Q., Rutherford, S.A., Low, B., Zhao, Z.J., 2005. Inactivation of src family tyrosine kinases by reactive oxygen species in vivo. J. Biol. Chem. 280, 23918–23925.

Tang, V.W., 2006. Proteomic and bioinformatic analysis of epithelial tight junction reveals an unexpected cluster of synaptic molecules. Biol. Direct 1, 37.

Tatapudi, P., Fenton, J.M., 1993. Synthesis of hydrogen peroxide in a proton exchange membrane electrochemical reactor. J. Electrochem. Soc. 140, L55–L57.

Uhland, S.A., 2003. Implantable biomems for drug delivery. In: MRS Spring Meeting , San Franscisco. Materials Research Society.

Uhland, S.A., Polito, B.F., Maloney Jr., J.M., Sheppard, N.F., Herman, S.J., Yomtov, B.Y., 2004. Controlled release device and method using electrothermal ablation.

Utech, M., Mennigen, R., Bruewer, M., 2010. Endocytosis and recycling of tight junction proteins in inflammation. J. Biomed. Biotechnol. 2010, 484987.

Waters, C.M., Savla, U., Panos, R.J., 1997. KGF prevents hydrogen peroxide-induced increases in airway epithelial cell permeability. Am. J. Physiol. Lung Cell. Mol. Physiol. 272, L681–689, http://ajplung.physiology.org/cgi/reprint/272/4/L681.pdf.

Xie, J., Miao, Y., Shih, J., He, Q., Liu, J., Tai, Y.C., Lee, T.D., 2004. An electrochemical pumping system for on-chip gradient generation. Anal. Chem. 76, 3756–3763, PMID: 15228351. http://pubs.acs.org/doi/pdf/10.1021/ac035188u.